

# Lipid Domain Theory of General Anesthesia

Honors Thesis in Biophysics

---

Ellyn Gray

**APRIL 2013**

Research Advisor:

Dr. Sarah Veatch

[sveatch@umich.edu](mailto:sveatch@umich.edu)

University of Michigan

# Abstract

There is a long-standing debate whether general anesthetics act through non-specific perturbation of bilayer physical properties or through binding to specific sites within ion channels, particularly the GABA<sub>A</sub> receptor. In this study, we investigate how a series of liquid general anesthetics impact phase transition temperatures in giant plasma membrane vesicles (GPMVs) isolated from RBL-2H3 mast cells. We have chosen to use a series of alcohol general anesthetics with a range of hydrophobic chain lengths and well-characterized anesthetic potencies. We find that all alcohols investigated lower critical temperatures in GPMVs. When alcohol concentrations are scaled by anesthetic potency, the magnitude of depression is equivalent within error. All compounds depress critical temperatures by  $4\pm 1^\circ\text{C}$  when added to vesicles at their anesthetic dose. This is larger than depressions previously measured for the gel-liquid transition in vesicles. Additionally, the same  $4\pm 1^\circ\text{C}$  shift in phase transition temperature is observed for other clinically used anesthetics, including phenylethanol, indicating that these diverse compounds could act in a non-specific manner through influencing membrane domain formation.

# Chapter 1

## Introduction

### 1.1 Membrane structure

Cell plasma membranes are structured according to the ‘fluid mosaic model,’ with a two-dimensional lipid bilayer separating the inner and extracellular environments and interspersed globular proteins and oligosaccharides.<sup>1</sup> Membrane lipids are amphipathic molecules characterized by a hydrophilic head group on the surface of the bilayer and hydrophobic groups or fatty acid chains on the inside. These lipids include phospholipids, glycolipids, and cholesterol. Phospholipids are the primary lipid in the membrane and contain two hydrophobic fatty acid chains. Cholesterol plays multiple important roles: it acts to reduce membrane fluidity, inhibit the formation of gel or solid phases, and is required for formation of the liquid-ordered membrane phase described below.<sup>2</sup> Non-covalent hydrophobic interactions hold the lipids together; however, the structure is still quite fluid, and phospholipids and proteins are free to diffuse laterally across the surface. Additionally, the membrane is coupled to cortical cytoskeleton, which impacts the diffusion rates and localization of lipids and integrated proteins.<sup>3</sup>

## 1.2 Phase separation and lipid domains

The lipid bilayer is a heterogeneous mixture of numerous lipids and can exist in several different phases, both in cell membranes and in bilayers made from purified components. In the gel phase, lipids are packed tightly to the point where they are not free to diffuse laterally. In the liquid ordered phase, lipids undergo rapid lateral and rotational diffusion while being moderately well packed, which is facilitated by the presence of cholesterol. The liquid disordered phase is characterized by loosely packed lipids, which frequently have higher degrees of unsaturation, and hence more ‘kinks’ that prevent tight packing.<sup>4</sup> Lipid bilayers containing a single lipid species that experiences a phase transition between liquid-disordered and gel phases at a specific temperature called the chain melting temperature ( $T_M$ ). Multicomponent membranes can also experience a miscibility transition, where the membrane passes from a uniform single phase at higher temperature to two distinct phases at lower temperatures, either gel and liquid, or liquid-ordered and liquid-disordered.

Mammalian cell plasma membranes isolated from cortical cytoskeleton are composed of a special ‘critical composition’ at which they pass through a critical temperature ( $T_c$ ).<sup>5</sup> Above  $T_c$ , the membrane exists as a single, yet heterogeneous liquid phase. Within a few degrees of  $T_c$ , micron-sized composition fluctuations are observed when isolated plasma membrane vesicles are imaged using fluorescence microscopy. Super-critical fluctuations increase in size and magnitude as temperature is lowered from the uniform phase. Just below the critical temperature, two distinct phases are visible vesicle surface, but fluctuations are observed at domain boundaries. At low temperatures, vesicles completely separate into two phases, with roughly half the vesicle surface occupied by each phase. Figure 1.1 shows a vesicle passing

through this transition temperature. As temperature decreases, the domains (fluorescently labeled bright and dark phases) become larger.

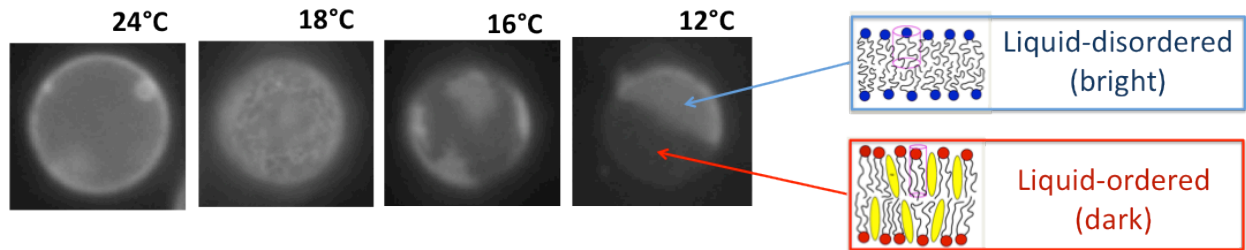


**Figure 1.1** A fluorescently labeled giant plasma membrane vesicle as it passes through a phase transition temperature. The liquid-disordered phase is fluorescently labeled while the liquid-ordered phase is not. At 24°C the membrane is one uniform phase, but as the temperature decreases towards 16°C domains are clearly visible. At 12°C the membrane is completely phase separated into two distinct hemispheres.

Critical fluctuations in purified model membranes and isolated biological membranes are successfully modeled using a two-dimensional Ising model, where each phase is represented by one of two spin states (+1 or -1) and each spin in the lattice interacts with its nearest neighbors. When spin states are parallel, energy is minimized; therefore, it is more energetically favorable for particles with like phases to associate with one another.<sup>6</sup> As the system's free energy is minimized, the Ising model lattice will fluctuate towards a phase separated conformation. The loss in free energy due to a decrease in entropy can be accounted for by the increase in free energy from bringing together particles with lower interaction energies. There is a balance between entropy and energy that controls the size and lifetime of membrane domains. Above  $T_c$ , entropy wins and compositional heterogeneity within the membrane remains small and short lived. Below  $T_c$ , energy wins and spins organize into macroscopic phase separated domains. Near  $T_c$ , these two contributions are nearly balanced, allowing for the formation of large and dynamic fluctuations.

Using this model, previous work has shown that the actin skeleton acts as ‘pinning sites’ on the plasma membrane to disrupt larger fluctuations and instead localizes one phase to form a network of channels, segregating the membrane.<sup>7</sup> This work has led to the hypothesis that the plasma membranes of intact cells are unable to fully phase separate but rather form structures on the length-scale of the cortical meshwork that may have significance in membrane component transport across the membrane. Because one of our goals is to observe phase separation in membrane, interference by the actin cytoskeleton would be counterproductive. We therefore use giant plasma membrane vesicles (GPMVs) or blebs as a model membrane. Blebs are vesicles formed from a cell membrane that is no longer coupled to the actin cytoskeleton. They retain the lipid and protein composition of the original cell and therefore act as a very practical model of phase behavior in membranes. Phase transition temperatures in mammalian blebs are typically observed to be from 15 to 25°C and often the phase transition involves the formation of domains separating the bleb into two distinct regions. The two phases can be imaged using fluorescence microscopy a fluorescent dye that partitions specifically into one particular phase. Figure 1.2 shows fluorescently labeled blebs still attached to cells. While the bleb can phase separate into large domains, adjacent regions of intact cell remain unstructured on the micron-scale even though they presumably have the same plasma membrane composition.

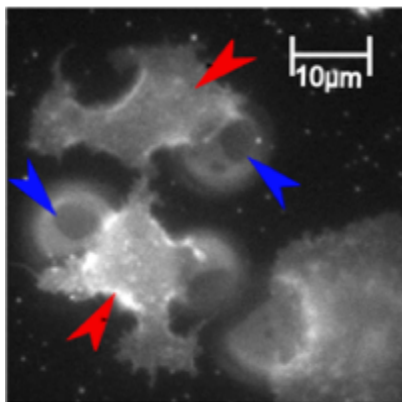


**Figure 1.2** Blebs attached to rat basophilic leukemia cells. Blebs are marked with blue arrows and cells are marked with red arrows. The membranes are labeled with DiI-C12. Figure reproduced from: Machta BB, Papanikolaou S, Sethna JP, Veatch SL (2011). *Biophys. J.* **100**:1668-1677.

## **1.3 History of the mechanism of general anesthesia**

General anesthetics have been used to induce a reversible loss in consciousness during surgery since the mid-1800s. However, for over 150 years, their mechanism of action has remained largely unknown. Paul Ehrlich first proposed the concept of specific interactions between drugs and their targets<sup>8</sup>; however, this idea has been a large subject of debate for the past few decades.

### **1.3.1 Meyer-Overton Correlation**

General anesthetics include different classes of molecules with a large structural variety, yet very similar effects in the induction of anesthesia<sup>9</sup>. Because of this, it has been argued that anesthesia likely does not occur through specific binding to proteins since it would require binding sites for many structurally diverse molecules. In the beginning of the twentieth century, HH Meyer and CE Overton experimentally supported a new idea: non-specific interactions between general anesthetics and the lipid membrane component of cells.<sup>10</sup> Research conducted by Meyer and Overton (independently but at similar times) demonstrated a linear relationship between the general anesthetic partitioning in oil and water and the anesthetic potency of these molecules in the immobilization of tadpoles (Figure 1.3). They proposed that anesthesia was actually the result of a lipid-based mechanism.

### **1.3.2 Proposed lipid models for general anesthesia**

While the non-specific lipid membrane mechanism was investigated heavily in the first half of the twentieth century, it has fallen out of favor over roughly the past two decades. However, lipid membrane properties that have been investigated with anesthetics include membrane curvature, thickness, and lateral pressure.<sup>11,12,13</sup> Recently, there has been a proposal that action potential

propagation requires significant structural changes in membrane lipids that is enabled by their proximity to a liquid-gel phase transition. In this model, general anesthetics act by lowering this transition temperature, thereby inhibiting the ability of membranes to undergo large density changes required for signal propagation.<sup>14</sup>

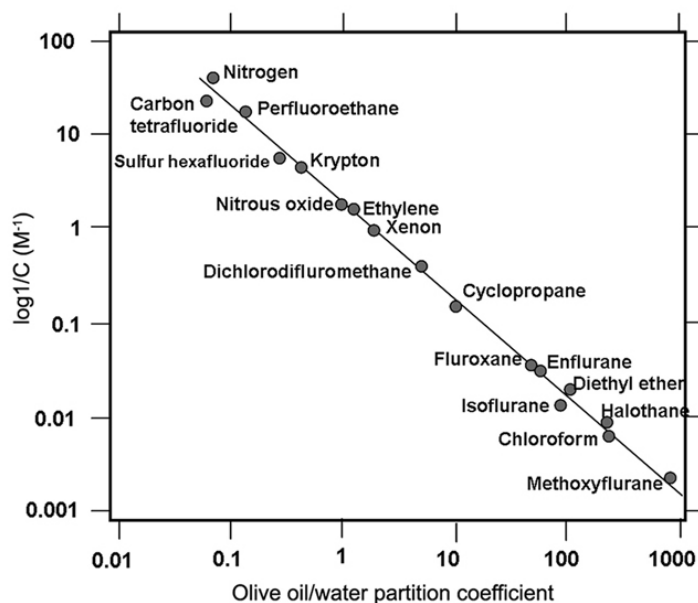


**Figure 1.3** Plot of anesthetic potency ( $\log[1/C]$ ) versus the olive oil: gas partition coefficient for various general anesthetics. Figure reproduced from: Favia AD (2011). *Frontiers Biosci.* **16**: 1276-1290.

### 1.3.3 Direct binding to proteins

More recently, effort has gone into exploring the existence of multiple binding sites for general anesthetics on receptors. One of the primary receptors involved in anesthesia is the GABA<sub>A</sub> receptor, a chloride ion channel whose primary ligand is  $\gamma$ -aminobutyric acid (GABA). GABA<sub>A</sub> is composed of five subunits of transmembrane helices, making it a very large membrane protein. When bound to GABA, the chloride pore of the receptor allows an influx of chloride ions, which hyperpolarizes the membrane to cause an inhibitory post-synaptic potential (IPSP) in neuronal cells. Therefore, in order to induce anesthesia, the mechanism would involve the



activation of the GABA<sub>A</sub> receptor to suppress the propagation of action potential. Previous research has investigated the possibility of specific binding sites on GABA<sub>A</sub> for general anesthetics<sup>15</sup>. The location of these binding sites in nicotinic acetylcholine receptors (nAChR), and more recently GABA<sub>A</sub> receptors, was found using photoactivatable analogs of certain general anesthetics.<sup>16</sup> This binding has been proposed to cause an allosteric regulation of the receptor functioning.

### **1.3.4 Lipid domains in general anesthesia**

Based on research even in the past few years, it is clear that the spectrum of theories for the mechanism of general anesthesia is still quite broad. We aim to develop a model that incorporates the importance of both protein signaling and regulation by lipids by proposing a new way of thinking about how we can influence the membrane. One specific property that we study is the formation of lipid domains, sometimes referred to as ‘lipid rafts’ in cellular membranes. It has been proposed that the formation of these lipid rafts has a functional role in key biological processes such as immune signaling and endocytosis. We use general alcohol anesthetics, which are n-alcohols that partition into the membrane by a level related to the oil and water partitioning coefficient (unique to each alcohol). By studying the effects of these general anesthetics on the phase behavior of membranes and phase behavior relation to membrane receptor activity we aim to gain a better understanding of a possible allosteric mechanism of anesthesia.

# Chapter 2

## Methodology

### 2.1 Experimental set-Up

#### 2.1.1 Cell culture

In a 25 cm<sup>2</sup> cell culture flask, RBL (Rat Basophilic Leukemia)-2H3 mast cells are incubated at 37°C in 5% CO<sub>2</sub> and are passaged using 0.25% Trypsin/EDTA and RBL media 24 hours prior to the blebbing process. The media is prepared with 800 mL MEM 1X with L-glutamine and earle salts, 200 mL fetal bovine serum, and 1 mL gentamicin. Trypsin/EDTA and the RBL media are warmed to 37°C. Cells are then washed with 2 mL Trypsin/EDTA and left to sit at 37°C for five minutes with 2 mL Trypsin/ EDTA. After the cells no longer adhered to the flask, they were centrifuged at 500 rev/min for five minutes with 8 mL of additional media and the pellet was then resuspended in an appropriate amount of media for a final concentration of 10<sup>6</sup> cells/mL. About 5×10<sup>6</sup> RBL cells were plated in each new flask and doubled in concentration overnight.

#### 2.1.2 Preparation of labeling buffer

To prepare the labeling buffer, 2 μL DiI-C12 (Invitrogen) at a concentration of 10 mg/mL in methanol (Sigma Aldrich) is added to 100 mL methanol. 100 μL of the solution is then added to

10 mL bleb buffer. DiI-C12 is a fluorescent dye that has an extinction coefficient of  $150,000 \text{ M}^{-1} \text{ cm}^{-1}$  and is excited by 532 nm light. When viewed under the microscope, it partitions strongly into the liquid-disordered phase. This allows for the imaging of a distinct light phase and dark phase when vesicles are phase separated.

### **2.1.3 Preparation of active buffer**

To prepare the active buffer, 15 mg dithiothreitol (DTT) (Sigma Aldrich) is dissolved in 100 mL of 36% formaldehyde (Fisher Scientific). This is vortexed for a few seconds until the DTT is completely dissolved in formaldehyde. 20 mL of this solution was added to 10 mL bleb buffer for a final concentration of 0.3 mg/mL DTT.

### **2.1.4 Blebbing**

The process of blebbing involves chemically interfering with cell functioning in a manner such that parts of the cell membrane detach from the cytoskeleton and pinch off to form vesicles containing cytoplasm. Bleb buffer is prepared as a 1 L stock solution with water and 150 mM NaCl, 2 mM  $\text{CaCl}_2$ , and 20 mM HEPES. The solution is set to a pH of 7.4. RBL cells are washed twice with bleb buffer and then 1 mL of the labeling buffer is added. The cells are left to shake at 100 rev/min for five minutes at  $37^\circ\text{C}$ . After the cells have labeled, they are washed twice with bleb buffer, once with active buffer, and then 1 mL of active buffer is added to the flask. The cells are left to shake at 100 rev/min for one hour. After one hour, the blebs are floating in the buffer and extracted from the flask with a pipette, without disturbing attached cells.  $20 \mu\text{L}$  of this volume is pipetted onto a cover slip lined with thin layer of vacuum grease along the edges of the slip. A second cover slip is used to form a sealed chamber. For a higher density of blebs, the

vacuum grease can be applied thicker so as to allow a greater number of blebs per unit area after the blebs sink to a single plane of view.

## 2.1.5 Application of general anesthetics

After blebs are extracted from the incubator, they are treated with various concentrations of general alcohol anesthetics based on the alcohol AC<sub>50</sub> values specified in Pringle *et. al.*<sup>17</sup> (Table 2.1) and multiples of these values. These concentrations were determined using n-chain length alcohols to treat tadpoles, which have a ‘righting reflex’ used to properly orient themselves. The AC<sub>50</sub> concentration was defined to be the concentration at which 50% of tadpoles lost this reflex.

| <i>Anesthetic potency of alcohols in tadpoles at room temperature</i> |                      |                                    |
|---|----------------------|------------------------------------|
| <b>Alcohol</b>  | <b>C<sub>n</sub></b> | <b>ED<sub>50</sub> ± SE</b>        |
|   |                      | <b>M</b>                           |
| <b>Ethanol</b>  | <b>2</b>             | <b>0.12 ± 0.01</b>                 |
| <b>Propanol</b>   | <b>3</b>             | <b>5.4 ± 0.6 × 10<sup>-2</sup></b> |
| <b>Butanol</b>  | <b>4</b>             | <b>1.2 ± 0.1 × 10<sup>-2</sup></b> |
| <b>Hexanol</b>  | <b>6</b>             | <b>7 ± 1 × 10<sup>-4</sup></b>     |
| <b>Octanol</b>  | <b>8</b>             | <b>6 ± 0.9 × 10<sup>-5</sup></b>   |
| <b>Decanol</b>  | <b>10</b>            | <b>1.3 ± 0.2 × 10<sup>-5</sup></b> |
| <b>Dodecanol</b>  | <b>12</b>            | <b>5.4 ± 0.9 × 10<sup>-6</sup></b> |

**Table 2.1** Concentrations used as AC<sub>50</sub> values for n-alcohols, determined using tadpoles. Table reproduced from: Pringle MJ, Brown KB, Miller KW (1981). *Mol. Pharmacol.* **19**: 49-55.

In general, as chain length increases, potency increases and the concentration used is smaller.

Alcohols include ethyl alcohol (AC<sub>50</sub>=120mM), isopropanol (AC<sub>50</sub>=54mM), octanol (AC<sub>50</sub>=60μM), and decanol (AC<sub>50</sub>=13μM). All n-alcohols are purchased from Sigma Aldrich.

Phenylethanol was also applied to blebs as a clinically used anesthetic, and the AC<sub>50</sub> concentration is estimated to be 20 mM based on previous studies.<sup>18,19</sup> For a given sample of blebs, the alcohol is diluted in a volume of bleb buffer so that the bleb density remains constant.

The blebs are incubated with the alcohol for five minutes and then immediately applied to the slide for imaging.

### **2.1.6 Microscope**

The Olympus IX81 microscope was used to image the bleb samples. Light was from an Olympus U-RFL-T power source, which passes through a filter (selects for  $535\pm 25\text{nm}$  excitation and  $610\pm 33\text{nm}$  emission wavelengths) and a 40X objective. The temperature of the sample was controlled using a home built Peltier device based stage and a temperature controller from Oven Industries. Cover slips were adhered to the stage using Arctic Alumina Premium Ceramic Polysynthetic Thermal Compound or Arctic Silver 5 High-Density Polysynthetic Silver Thermal Compound.

## **2.2 Data acquisition**

Images samples are viewed with an Andor Neo Camera using Andor SOLIS software. The display was set to min/max mode and acquisition time between 0.01 and 0.15 seconds. Blebs were imaged at temperatures ranging from  $25^{\circ}\text{C}$  to  $10^{\circ}\text{C}$  in increments of 2 or  $3^{\circ}\text{C}$ . Near the phase transition temperature data was acquired in smaller temperature intervals. At each temperature, about 200 to 500 blebs were imaged (about 10 frames as shown in figure 2.1) in which the plane of focus was on the membrane surface for the majority of blebs. It was also confirmed for each frame that the majority of blebs could be distinguished as being ‘phase separated’ (two-phase) or ‘non-phase separated’ (one-phase). Images were saved in individual files for each temperature.

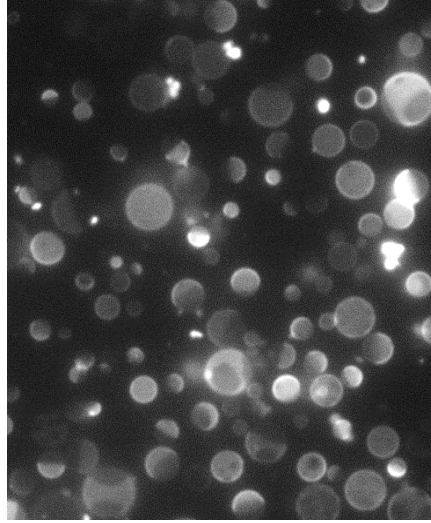


**Figure 2.1** Image of a field of blebs in which almost all blebs can be unambiguously labeled as one phase or two phases.

## 2.3 Data analysis

Data was analyzed using the MatLab program ‘count\_vesicles’. In this program, at each given temperature of a sample the program runs through all frames and the user right-clicks for non-phase separated vesicles and left-clicks for phase separated vesicles (Figure 2.2, left panel). Phase separation is defined as the presence of a distinct light and dark phase in a single vesicle. Right-clicked vesicles are tagged with a yellow marker and left-clicked with a red marker to prevent the double counting of vesicles. The program creates a histogram plot for these two states at each temperature. After this procedure is followed, the program ‘plot\_countdata’ is used to fit the data to a sigmoidal curve (equation 2.1) with fit parameter B showing the percentage of phase-separated vesicles versus temperature.  $T_M$ , the phase transition temperature, is determined to be the point at which fifty percent of vesicles are phase separated.

$$\%Separated = 100 \times \left(1 - \frac{1}{1 + e^{(T-T_M)/B}}\right) \quad (2.1)$$

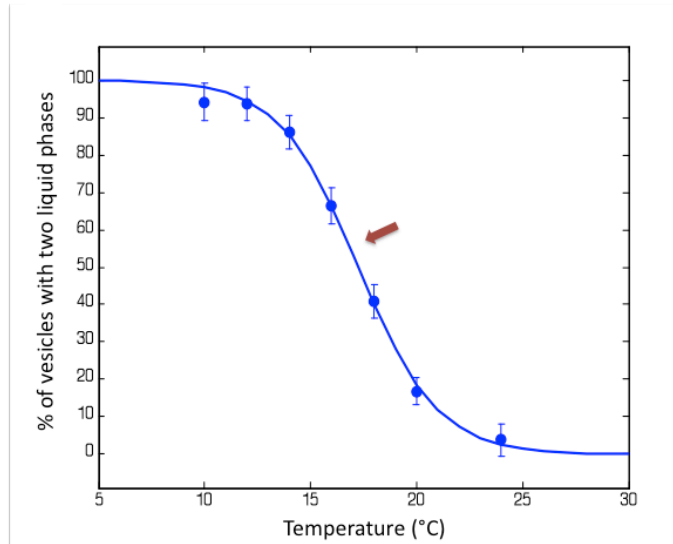
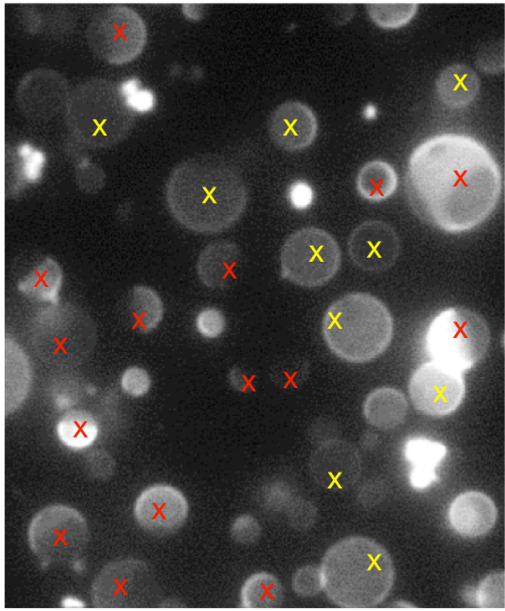


**Figure 2.2** (left) Field of blebs in which phase separated blebs are labeled with a red marker and non-phase separated blebs are labeled with a yellow marker. (right) Sigmoidal curve fit showing the percentage of phase separated vesicles over a range of temperatures. The transition temperature,  $T_M$ , is marked at the point where 50% of vesicles are phase separated (red arrow).

The right panel of Figure 2.2 shows the resulting sigmoidal curve, with error bars defined as  $100/\sqrt{N-1}$  where  $N$  is the number of vesicles counted for each temperature.

# Chapter 3

## Results

Our results for the following experiments involve the calculation of phase transition temperature shifts from that of a control with no alcohol treatment. While a typical control sample has a transition temperature between 18-20°C, there is significant day-to-day variation for transition temperatures measured in untreated blebs. Therefore, temperature shift is measured against a control of blebs from the same cell sample from a single day.

### 3.1 Effect of variable alcohol concentration

For each alcohol tested, we used multiples (typically 0.5, 1, 2, and 5) of the alcohol's  $AC_{50}$  value. In ethanol, the  $AC_{50}$  value is 0.12 M and we used concentrations of 0.06, 0.12, 0.24, and 0.6 M. We find that at a given temperature, the presence of the anesthetic decreases the ratio of phase-separated vesicles, as seen in figure 3.1. This is most pronounced in the temperature range surrounding  $T_M$ . In a 1X concentration of any alcohol used, we notice a  $T_M$  shift of about 4°C. At the phase transition temperature of untreated blebs, the addition of a 1X concentration of ethanol lowers the percentage of phase-separated blebs from 50% to about 15%.



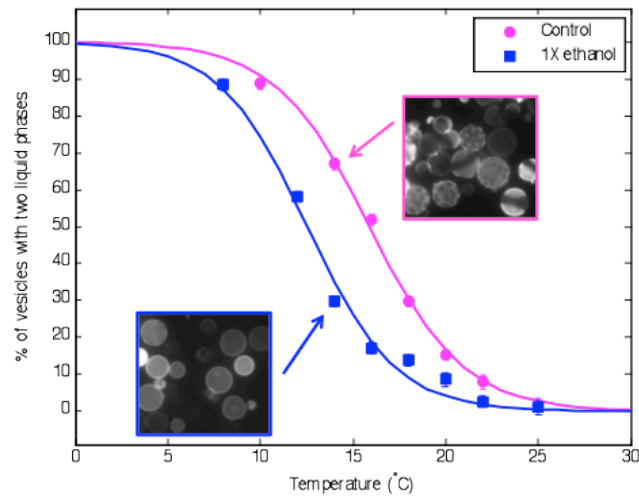


**Figure 3.1** Phase separation diagram for a 1X concentration of ethanol and a control sample. In the control (pink), more blebs are phase separated at 14°C than in the sample treated with ethanol.

In ethanol and all other alcohols used, we find that increasing the concentration of anesthetic decreases the temperature at which blebs phase separate. Figure 3.2 displays this effect for ethanol.

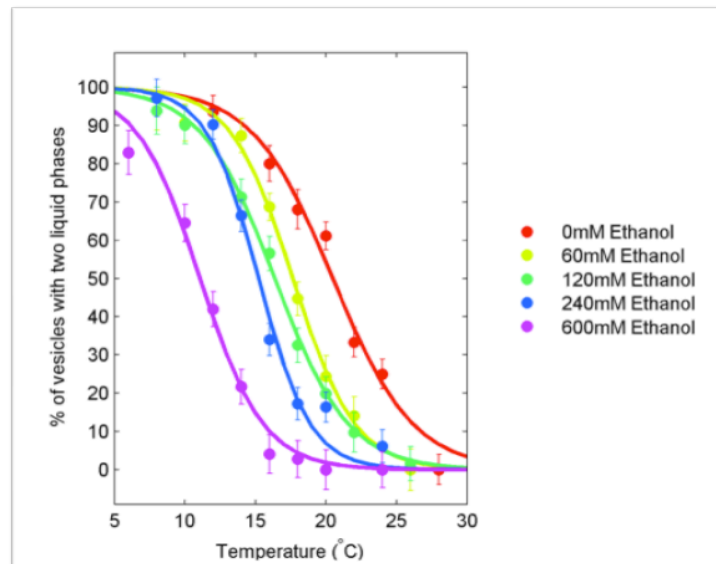


**Figure 3.2** Sigmoidal curve fits for five different concentrations of ethanol in a single sample. As the concentration of ethanol increases, phase transition temperature decreases.

## 3.2 Effect of variable alcohol concentrations for all alcohols

In a comparison of all alcohols used for these experiments, we plot the  $T_M$  shift at the concentrations used. The plotted values are an average of all shifts measured for a given concentration of alcohol. In octanol and decanol data sets, the  $AC_{50}$  values and concentrations used are very small compared to those of ethanol and propanol due to the potency of longer-chained alcohols and preference for a non-polar phase. In figure 3.3, this data will therefore appear as a straight, vertical line.

Dimethyl Sulfoxide (DMSO) is not recorded to have any anesthetic effect yet it is a good solvent for some lipids and is therefore used as a control for these experiments. This ensures that the effect we see by increasing alcohol concentration is specific to general anesthetics and not just any molecule that can perturb the membrane. For the purposes of these experiments, we use a concentration of DMSO equivalent to one times and five times the  $AC_{50}$  value of ethanol. DMSO is known to mix with both polar and non-polar substance fairly well and should therefore be able to integrate into the membrane to some degree at these high concentrations. We find that the temperature shift measured by adding DMSO is negligible and at five times the  $AC_{50}$  ethanol value, the temperature shift is within error of  $0^\circ\text{C}$ .

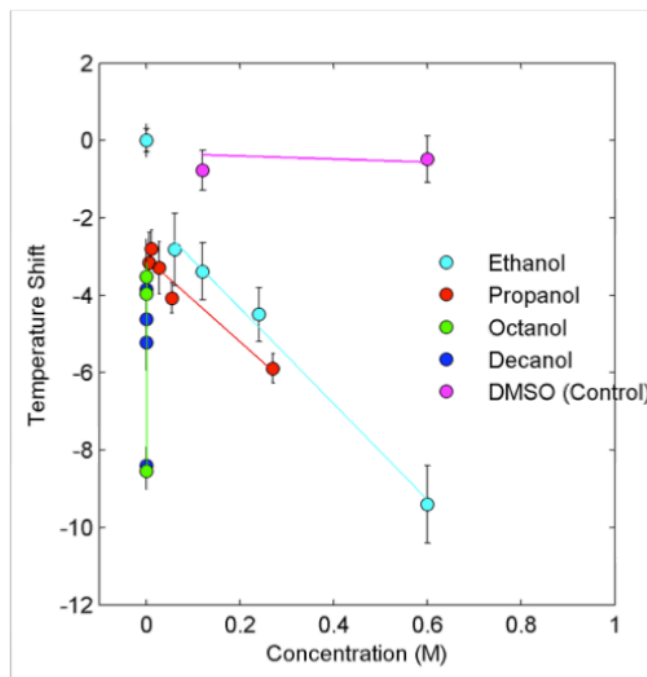


**Figure 3.3** Temperature shifts and linear fit for alcohol anesthetics and DMSO (non-anesthetic) for multiples of the specified  $AC_{50}$  concentrations.

### 3.2.1 Scaling of data to $AC_{50}$ values

By using  $AC_{50}$  values, the potency (partitioning into the membrane and relative anesthetic effect) of different chain length alcohols is accounted for, which is important given that potency varies by several orders of magnitude. In order to relate the temperature shift observed for general alcohol anesthetics, we scale the concentrations by the  $AC_{50}$  values so that the amount of alcohol used is now in terms of 1X, 2X, 5X, etc. In doing so, we find that the temperature shifts for all alcohols are very well correlated and there is a linear relationship between the temperature shift and the concentration divided by the  $AC_{50}$  value (shown in figure 3.4).

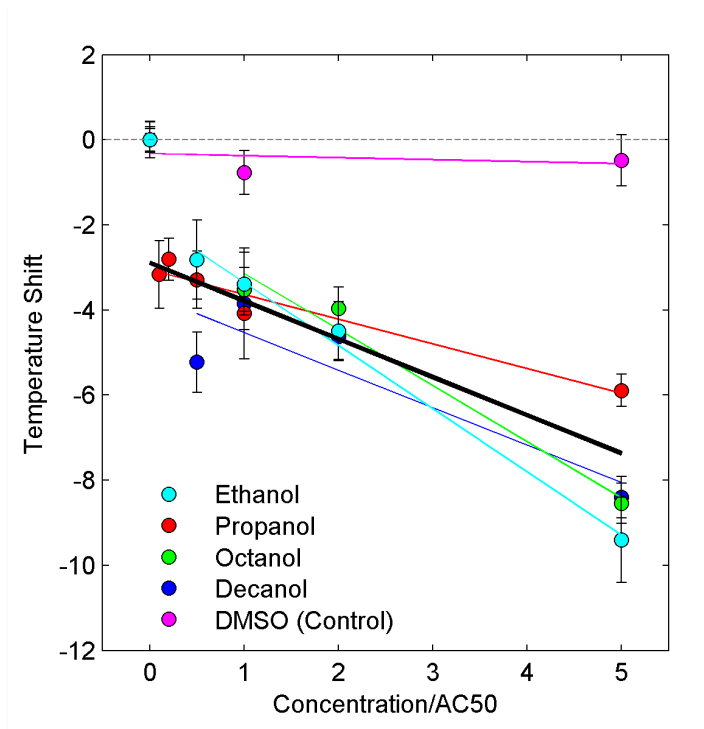


**Figure 3.4** Reconstruction of figure 3.3 with concentration scaled against the  $AC_{50}$  value for each particular alcohol anesthetic. The black line indicates a linear fit to the average temperature shifts for all alcohol anesthetics.

### 3.3 Nonlinear behavior at low anesthetic concentration

While we do observe a linear trend in transition temperature shifts for concentrations approaching the anesthetic dose, this line intercepts at about  $-2^{\circ}\text{C}$ , which is not consistent with the fact that there is no temperature shift with no alcohol added. In order to test what happens around this intercept, we used small concentrations of propanol ( $10^{-1}\text{X}/5.4\text{mM}$ ,  $5 \times 10^{-2}\text{X}/1.8\text{mM}$ , and  $10^{-2}\text{X}/0.54\text{mM}$ ). The results, shown in figure 3.5, demonstrate that in this range there is exponential behavior leading to an intercept at  $0^{\circ}\text{C}$  and a steep increase in phase transition temperature depression leading up to  $0.5\text{X}$ .

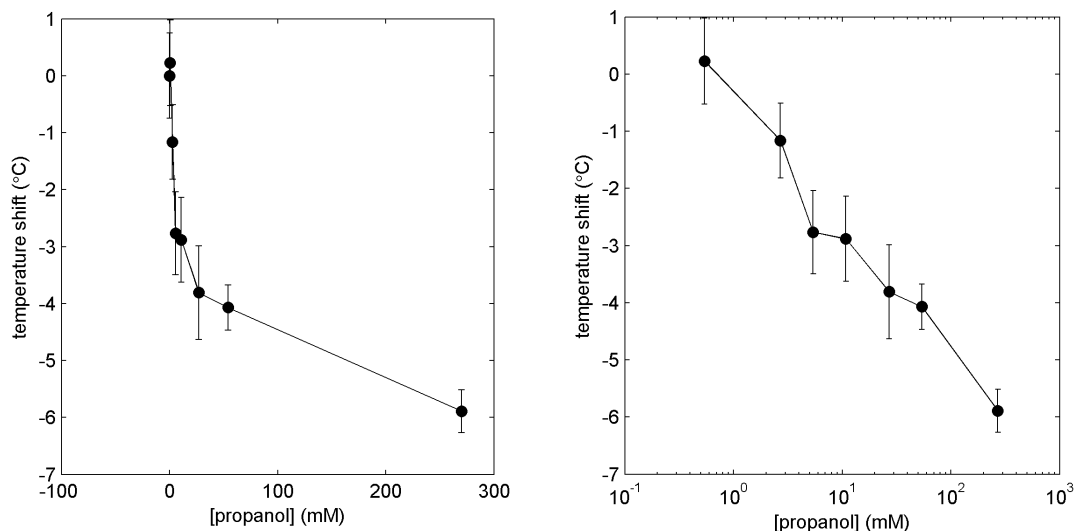


**Figure 3.5** Phase transition temperature shift plotted against propanol concentration on a linear scale (left) and logarithmic scale (right) to show non-linear behavior.

### 3.4 Using other anesthetics

In order to see if the lowering of phase transition temperature extends to a broader range of general anesthetics, we treated our system with phenylethanol (PEtOH). PEtOH is a local anesthetic commonly used in surgeries. It is a small molecule consisting of an alcohol group at the end of an aromatic ring and two-carbon chain, and it could orient itself within the lipid membrane with the ring on the internal hydrophobic side. Previous studies have investigated alternative mechanisms of anesthesia with this compound, including helix aggregation.<sup>20</sup> Upon a linear fit of the data, it was found that a clinical concentration of PEtOH (20 mM) would decrease the phase transition temperature by about 3-4°C when applied to the blebs, as was observed with the AC<sub>50</sub> concentrations of general alcohol anesthetics. Additionally, the fit line features a non-zero negative intercept of about 1-2°C, as was observed with other n-alcohols, indicating it likely has a similar non-linear pattern at smaller concentrations. Figure 3.6 shows the change in phase transition temperature upon the addition of PEtOH, which reveals the same pattern seen for the n-chain length alcohols.

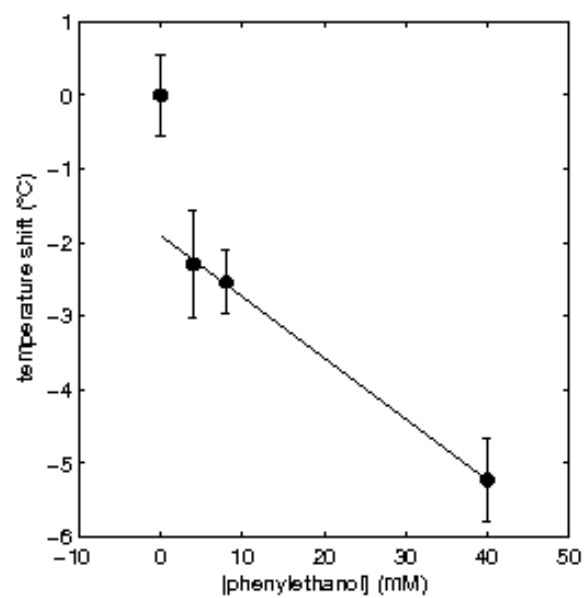


**Figure 3.6** Temperature shifts for different concentrations of PEtOH and the linear fit of this model data.

# Chapter 4

## Discussion

### 4.1 Relationship to lipid theory of general anesthesia

In this study, we demonstrate that the addition of liquid n-alcohol general anesthetics induces a depression in critical temperatures by several degrees, and the temperature shift is proportional to the concentration of alcohol applied. Furthermore, the temperature shifts for all n-alcohols scale by the anesthetic dose. This effect was not unique to n-alcohols, as the addition of clinically relevant concentrations of phenylethanol was also able to induce a similar phase transition temperature decrease in blebs. These similarities suggest that the membrane can act as a non-specific system to accommodate a variety of conformations, and phase transition temperature is influenced to a similar degree amongst general anesthetics. A gel-liquid transition has previously been studied with general anesthesia, although in this case only a small ( $<1^{\circ}\text{C}$ ) temperature shift is observed.<sup>15</sup> Our measured transition temperature decrease of 3-4 $^{\circ}\text{C}$  is significantly greater than that of the gel-liquid shift, and it may be large enough to induce some sort of allosteric effect on membrane components involved in anesthesia. Having a strong relationship between transition temperature shift and anesthetic potency supports the hypothesis that lipid-mediated heterogeneity arising from the miscibility critical point has some mechanistic role in anesthesia.

There are several possible methods by which the alterations in phase separation and domain formation could be regulating membrane components, specifically the GABA<sub>A</sub> receptor. Based on our findings, it is likely that the receptor is sensitive to its lipid environment, particularly some property of the ordering of lipids. One distinguishing feature between the two liquid phases of lipids is the presence of cholesterol in the liquid ordered phase. An energetically favorable interaction between cholesterol and a closed, non-conducting state of the receptor may increase the probability of the inactive state existing within a two-phase system, where it can be surrounded by a higher density of cholesterol. The combination of this interaction and a physical preference for closing due to tighter packing in a liquid-ordered environment may reduce anesthesia in a phase-separated system. This would correlate well with our results given that alcohols reduce phase-separation for a given temperature, thereby reducing the presence of the inactive state of a GABA<sub>A</sub>-like receptor.

## **4.2 Phase transition temperatures with non-anesthetics**

One common argument against the possibility of a lipid-based mechanism of general anesthesia is the ‘cut-off effect’ that occurs with n-chain length alcohols. Although these alcohols increase in potency as chain length increases, after tridecanol there is no longer an anesthetic effect, despite the fact that the alcohols are still partitioning into the bilayer. The concept of a molecule having no anesthetic effect while still existing in the bilayer is mirrored by the treatment with DMSO. This molecule is an amphipathic molecule that quickly integrates into the membrane, reaching an equilibrium membrane concentration in about 3 ns.<sup>21</sup> For our experiments we used the same concentrations as those used for ethanol, since the partition coefficient is lower than that of the longer chained alcohols and it has a slight preference for the hydrophilic phase.



DMSO has not been reported to induce anesthesia, and the fact that there was no significant change in transition temperature using these molecules suggests that the transition between one and two liquid phases and the formation of domains may be a valid explanation for general anesthesia.

### **4.3 Implications in cell signaling**

Using GPMVs, it was shown that the addition of general alcohol anesthetics destabilizes the existence of lipid domains in plasma membranes by lowering the temperature at which they become more distinct. Energetically speaking, they increase the entropy of the system so that it overcomes enthalpic effects at lower temperatures. Using the data collected, we propose that the phase behavior of membranes can allosterically regulate the activation of receptors such as the GABA<sub>A</sub> receptor. Because anesthesia is induced when GABA<sub>A</sub> is in an active, conducting state, the active state of this receptor would preferentially exist when the membrane is in a uniform, single phase. This may be due to coupling effects between the receptor and its neighboring lipid environment. In order to study this, we will explore the free energy of the system for the inactive and active receptor in a one-phase and two-phase Ising model. For a large protein of the same approximate size as GABA<sub>A</sub>, boundary conditions will be assumed such that the active state of the protein has no coupling to surrounding lipids, while the inactive state prefers one of either liquid ordered or liquid disordered lipids. Under these assumptions, the active state would have a lower minimum energy in a uniform membrane and the inactive state would have a lower minimum energy in a phase-separated system where it could be surrounded by a single lipid phase. This Ising model system would be used to predict whether the 4°C shift seen with the

addition of the  $AC_{50}$  dosage of each anesthetic is significant enough to induce 50% potentiation of the receptor.

In order to observe the effect of phase separation on receptor activation, future experiments can involve the expression of  $GABA_A$  or related receptors in blebbed cells in order to use the same non-actin coupled system. By analyzing the localization of the receptor in different phases during activation and inactivation we can understand how a receptor interacts with its lipid environment. Additionally, the relative levels of activation upon ligand addition at different temperatures can be measured to determine the efficiency of activation in different lipid environments. According to our model, it would be hypothesized that activation is more efficient at higher temperatures in a one-phase system. This one-phase environment is stabilized by the addition of general anesthetics, which means an inhibitory potential by an activated  $GABA_A$  channel is being generated.

Using fluorescence microscopy and RBL blebs, the phase separation of cell plasma membranes with a critical composition was observed. By applying this system to general alcohol anesthetics, it was found that alcohols lower phase transition temperature according to their partition coefficient and anesthetic potency. This correlation supports the concept that general anesthetics act in an allosteric manner by influencing lipid domain formation. Comparing the results of alcohol anesthetic experiments to future experiments with the Ising model and expressed receptors in blebs will provide further evidence in support of the lipid-phase domain theory of general anesthesia.

## References

---

- <sup>1</sup> Singer SJ, Nicolson GL (1972). *Science*. **175**:720-731.
- <sup>2</sup> Veatch SL, Keller SL (2005). *Biochim. et. Biophys. Acta*. **1746**: 172-185.
- <sup>3</sup> Kusumi A, et. al. (2012). *Annu. Rev. Cell. Dev. Biol.* **28**: 215-250.
- <sup>4</sup> Simons K, and Ikonen E (1997). *Nature* **387**: 569–572.
- <sup>5</sup> Veatch SL, Cicuta P, Sengupta P, Honerkamp-Smith A, Holowaka D, Baird B (2008). *ACS Chem. Bio.* **3**: 287-293.
- <sup>6</sup> Newman MEJ and Barkema GT (1999). Oxford New York: Clarendon Press; Oxford University Press. xiv: 475.
- <sup>7</sup> Machta BB, Papanikolaou S, Sethna JP, Veatch SL (2011). *Biophys. J.* **100**:1668-1677.
- <sup>8</sup> Weir, CJ (2006). *Contin. Educ. Anesth. Crit. Care Pain.* **6**: 49-53.
- <sup>9</sup> Meyer KH (1937). *Trans Faraday Soc.* **33**:1062–1068.
- <sup>10</sup> Meyer H (1899). *Naunyn-Schmiedeberg's Arch. Pharm.***42**:109-118.
- <sup>11</sup> Cantor RS (1997). *Biochem.* **36**: 2341-2344.
- <sup>12</sup> Franks NP, Lieb WR (1982). *Nature*. **300**: 487-493.
- <sup>13</sup> Gruner SM, Shyamsunder E (1991). *Ann. N. Y. Acad. Sci.* **625**: 685-697.
- <sup>14</sup> Heimburg T, Jackson AD (2007). *Biophys. J.* **92**: 3159-3165.
- <sup>15</sup> Lobo IA, Harris, RA (2008). *Pharmacol Biochem Behav.* **90**:90-94.
- <sup>16</sup> Forman SA, Miller KW (2011). *Can. J. Anaesth.* **58**: 191-205.
- <sup>17</sup> Pringle MJ, Brown KB, Miller KW (1981). *Mol. Pharmacol.* **19**: 49-55.
- <sup>18</sup> Wieslander A, Rilfors L, Lindblom G (1986). *Biochem.* **25**: 2511-2517.

---

<sup>19</sup> Seeman P (1972). *Parmaicol. Rev.* **24**: 583-655.

<sup>20</sup> Anbazhagan V, Munz C, Tome T, Schneider D (2010). *J. Molec. Bio.* **404**: 773-777.

<sup>21</sup> Gurtovenko AA, Anwar J (2007). *J. Phys. Chem. B.* **111**: 10453-10460.